

Experimentation And Optimization of Al-SiC based Metal Matrix Composite In Laser Micromachining

Tatwa Prakash Pattasani¹, Mukesh Kumar Panigrahi², Rugada Vaikunta Rao³

^{1,2}Assistant Professor, Department of Mechanical Engineering, Gandhi Institute For Technology (GIFT), Bhubaneswar

³ Assistant Professor, Department of Mechanical Engineering, Gandhi Engineering College, Bhubaneswar

Abstract- Aluminum silicon carbide is a MMC (metal matrix composite) largely used where strength to weight ratio & high thermal conductivity is primary in design criteria having wide application in Aerospace components, Automobiles & electronics industry. Present work deals in micro-grooving of this hard to machine material is carried out by diode pumped solid state pulsed Nd:YAG Laser. So optimal process parameter is highly required to get desired micro-groove with minimum deviation in upper, lower width & depth of groove. The experimental plan is carried out by CCD (central composite design) based on RSM (response surface methodology). The analysis of variance test is carried out to check the adequacy of the fitted regression mathematical models. Proper range of process parameters such as pulse width, pulse frequency, amount of current, assist air pressure were purposed. Screening test shows O₂ as assist gas when used .2 to 1 kgf/cm² pressure range gives best result because of its advantage during laser material interaction. The output responses selected for Analysis are upper width deviation, lower width & depth deviation of micro-groove produced on Al-SiC material. The interaction effect of different parameters on output response is analysing through response plots generated. Optimal process condition can be found out by utilizing meta-heuristic based search algorithm MOPSO (multi objective particle swarm optimization) technique. Applying this optimal process parameter values desired micro-grooves was machined under similar conditions. Machine grooves were machined by taking this optimized values.

Keywords – MMC, Nd:YAG, RSM, SEM, EDX

I. Introduction

Lasers are used in a wide range of applications to remove material, to join any type of material and also used in making very precise features where very high tolerance is the stringent requirement ([1],[2]). Small features can be made by these materials efficiently. These small features are very critical to the micro-electronics, aerospace, medical, renewable energy, automobile, and other industries. The machining of these small features is called laser micro-machining. Usually the feature size is less than 1 mm (less than 1mm) and the thickness of material also less than 1mm. The smallest attainable feature sizes are order of a micron [3]. Photons are the carrier of optical energy replacing electrons as the favourite tool in manufacturing industry. An important property of light is that it has no volume, photons have no charge, so when concentrated into a very small space, they do not repulse each other like negative charged electrons do. This is an important property especially for ultra short machining. Light moves through space as a wave, but when it incident on matter it behaves like a particle of energy, a photon. Keeping this in mind a high density optical energy beam is generated by stimulated emission [4] It has some inherent characteristics such as it is coherent, mono-chromatic and highly directional. These unique characteristics are useful in the processing of material. Moreover the emergence of advanced engineering materials, stringent design requirement, intricate shape and unusual size of work piece restrict the use of conventional machining methods. Also the problems with conventional mechanical micro-machining methods include unacceptable tool wear and force-induced damage on components. Laser micro-machining, being a non contact process, does not have the problem of mechanical damage and tool wear. Recent requirement with regard to the quality, flexibility, speed and production costs of the micro-machining process are becoming increasingly stringent. [5] The quality of surface and its microstructure mainly depends on how laser energy interact with material effectively. To release the electrons from the surface of the work material, it was required that the supply energy must be above its threshold level. This level of energy mainly depends on the absorptivity of the material towards laser beam energy. It was found that lasers in IR (infrared region) region best suitable for ablation in MMC composites. [6] To get stress free with high accuracy machined surface in MMC composites [7] DPSS Nd:YAG LASER with average power of 75w was used here. So the pulse duration is within nano- to milli secs which further reduces HAZ. This HAZ area can be reduced by effectively selecting the assist gas which can further helps in removing the molten material from the groove zone effectively. It was found that different gas with different properties react with material differently. Oxygen and nitrogen are reactive gases used for micro-machining of composite material. Oxygen is used as assist gas which reacts with

Al-SiC liberating heat energy. This reaction is especially exothermic in nature which produces heat energy that adds to the beam energy and acts as secondary source of energy ([8],[9],[10]). Nitrogen can be used to get high edge quality and shielding effect on the work piece material but due to economic aspect it is not recommended for this purpose.

II. Experimental Details

A. LASER MICRO-GROOVING PROCEDURE

Aluminium silicon carbide composite specimen having mean thickness of 4mm was used as work piece material. The machining was done by Nd:YAG laser emitting at different parameter setting as per the experimental planning. A CNC diode pumped Nd:YAG laser machining system which operated on pulsed mode & manufactured by M/s Sahajanand Laser technology, India. The detailed specification of the set up is listed on table-1. This system mainly consists of various subsystems such as beam delivery unit, power supply unit, Nd:YAG rod, oxygen air supply unit, cooling unit, RF Q-Switch unit and a CNC controller for X,Y,Z axis movement. Exact groove specification with desirable dimension was represented in the below diagram.

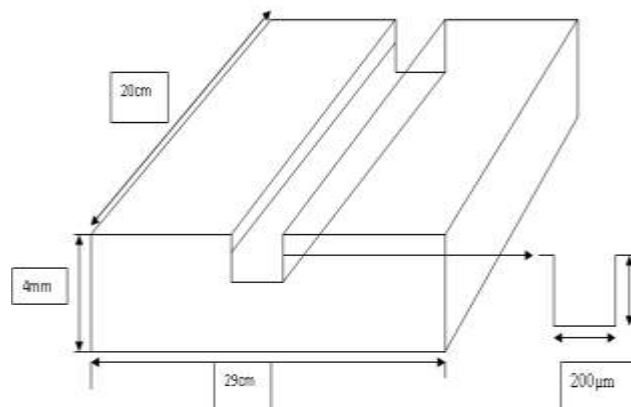


Fig.1 Schematic Diagram of a single groove (200x200)μm

TABLE I SPECIFICATIONS DETAILS OF DPSS ND-YAG LASER SETUP

Laser type & wavelength	DPSS Nd : YAG laser, 1064 nm
Mode of operation	Q-switched pulsed
Type of Q-switch used	Acousto-optic Q-switch
Mode of Laser Beam	Fundamental mode (TEM00)
Mirror reflectivity	Rear mirror 100% Front mirror 80%
Beam diameter	1 mm
Pulse width	120 ns
Spot diameter	21 μm

B. DESIGN OF EXPERIMENTS

The choice of an experimental design depends on the objectives of the experiment and the number of factors to be considered. In order to find the machining characteristics of the LASER beam micro-grooving on a flat AlSiC MMC work piece of 29 X 20 mm length and 4 mm thickness. The experimental scheme was designed by using Response Surface Method (RSM). RSM allows an estimate interaction and even quadratic effects[11].

The factors considered were diode current, pulse frequency, pulse width and air pressure. Central composite half design (CCD) with 30 runs was selected with an alpha value of 2.000. CCD is a very efficient method for fitting a second-order model. Experiments were carried out based on the design with 6 centre points. Four factors with five levels were considered for experimental purpose. The ranges of each factor were decided after conducting some pilot experiments. The actual and coded values are given in the table 2. As well as the schematic diagram of the micro-groove is shown in fig. 1.

III. Response Surface Methodology

Response surface modeling has been made to establish the mathematical relationship between the responses and the various machini

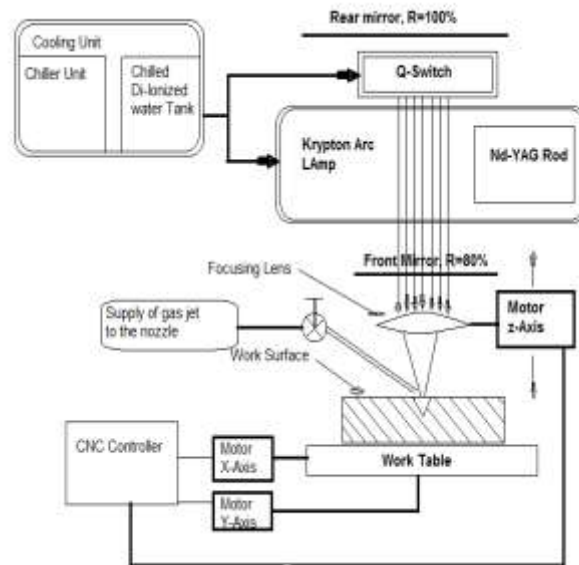


Fig.2 Schematic Representation of DPSS Nd:YAG Laser system Setup

TABLE 2 DIFFERENT UNITS OF ND:YAG LASER SETUP

Serial No.	Part Name
1	Beam Expander
2	Output Coupler
3	Aperture
4	Nd:YAG laser rod(4.1) with pumping diode(4.2)
5	Q-Switch Unit
6	Rear Mirror
7	CCD Camera
8	RF Q-Switch Unit
9	Chilling Unit
10	Work Table
11	Central Unit controlling the laser system
12	CNC Controller for XYZ movement
13	Co-axial Cylinder
14	Oxygen gas Cylinder
15	Bending Mirror
16	Focussing Lens

TABLE 3 ACTUAL&CORRESPONDING CODED VALUES FOR EACH PARAMETER

Parameters levels	-2	-1	0	1	2
Diode current(X1)	17	18	19	20	21
Pulse Frequency(X2)	2	3	4	5	6
Pulse Width(X3)	4	9	14	19	24
O₂ gas pressure(X4)	0.2	0.4	0.6	0.8	1

parameters. General second-order polynomial response surface empirical model, which is considered to analyze the parametric influences on the various response criteria, is as

follows:
$$Y_{dev.} = \beta_0 + \sum_{i=1}^n \beta_{ii} X_{iu} + \sum_{i=1}^n \beta_{ii} X_{iu}^2 + \sum_{i=1}^n \beta_{ij} X_{iu} X_{iu} + e_u$$

Where, Y_u is the corresponding response and the X_{iu} are coded values of the i th machining process parameters, the terms β_0 , β_i , β_{ii} and β_{ij} are the regression coefficients and the residual, e_u measures the experimental error of the u th observations. In the present set of analyses, the air pressure (X_1), diode current (X_2), pulse frequency (X_3) and pulse width (X_4) are considered as process parameters. Mathematical models of the responses have been established based on above equation using Design@EXPERT software by utilizing the experimental data as obtained from the designed experiment. The generated regression equation for upper width, lower width & depth deviation in design expert software given

as
$$Y_{DD} = -2.590 + .396X_1 + .2584X_2 - .1159X_3 + .01626X_4 - .0074X_1^2 - .00581X_2^2 - .00226X_3^2 + .000018X_4^2 - .04166X_1X_2 + .05447X_1X_3 + .01314X_1X_4 + .00489X_2X_3 - .001271X_2X_4 + .000164X_3X_4$$

$$Y_{LWD} = 1.391 + .259X_1 - .1229X_2 - .0304X_3 - .03644X_4 + .0019X_1^2 + .00286X_2^2 + .00017X_3^2 - .000163X_1X_2 - .0009X_1X_3 + .00415X_1X_4 + .00140X_2X_3 + .001501X_2X_4 + .000557X_3X_4$$

$$Y_{UPWD} = .225 + .061X_1 - .0327X_2 + .0315X_3 - .00591X_4 + .0416X_1^2 + .00107X_2^2 - .00510X_3^2 + .000043X_4^2 - .01181X_1X_2 + .01905X_1X_3 + .00224X_1X_4 + .00039X_2X_3 + .00380X_2X_4 - .000893X_3X_4$$

A. Analysis of Variance

The empirical models for the responses of upper width deviation, lower width deviation and depth deviation of the laser beam Micro-grooving on the Al-SiC work piece, analysis of variance (ANOVA) test has been done to explain which design parameters have a significant effect on the quality characteristic. All the responses were analyzed and it was found that R^2 value and Adj- R^2 value are laying above 85%. So the empirical developed model fits well.

TABLE 4 ANALYSIS of VARIANCE for DEPTH DEVIATION

Source	SumofS quares	df	Square	FValue	Prob > F
Residual	5.617	15	3.745		
Lack of Fit	3.334		3.334	0.73	0.6862
Pure Error	2.282	5	4.565	R^2	.96
R^2	.96			Adj- R^2	.93

TABLE 5 ANALYSIS of VARIANCE for UPPER WIDTH DEVIATION

Source	Sum of Squares	df	Mean Square	FValue	p-value Prob > F
Residual	1.381	15	9.204		
Lack of Fit	1.09	10	1.090	1.87	0.2530
Pure Error	2.907	5	5.814	R^2	.87
				Adj- R^2	.75

TABLE 6 ANALYSIS of VARIANCE for LOWER WIDTH DEVIATION

Source	SumofS quares	df	Square	FValue	Prob > F
Residual	6.278	15	4.125		
Lack of Fit	3.807	10	3.807	0.77	0.6616
Pure Error	2.471	5	4.941	R^2	0.85
				Adj- R^2	0.71

TABLE 5: VALUES OF OUTPUT RESPONSES

Exp No:	Upper Width(mm)	Lower Width(mm)	Depth deviation(mm)
1	0.0144	0.03173	-0.0091
2	0.00121	0.03157	-0.0414
3	0.0377	0.0246	0.0416
4	0.01534	0.03238	-0.0196
5	0.00831	0.04595	-0.0464
6	0.02399	0.04805	-0.0435
7	0.0277	0.04102	0.0104
8	0.0193	0.0175	-0.0097
9	0.0222	0.031	-0.0036
10	0.0235	0.0415	0.0127
11	0.0395	0.04166	-0.0128
12	0.03295	0.04434	-0.0028
13	-0.00201	0.02616	0.0591
14	0.00278	0.05903	-0.0144
15	0.02423	0.07187	-0.0042
16	0.03263	0.07834	-0.0205
17	0.0331	0.03173	-0.0027
18	0.02932	0.03044	-0.0024
19	0.01588	0.0351	-0.0554
20	0.0418	0.04926	0.0062
21	0.00928	0.02914	-0.0014
22	-0.000969	0.03375	-0.0194
23	0.027	0.0335	-0.0067
24	0.03077	0.06145	0.0074
25	0.03053	0.0482	-0.008
26	0.02447	0.0341	0.0021
27	0.023667	0.0292	-0.0038
28	0.0239094	0.0291	-0.0035
29	0.0232632	0.0294	0.0115
30	0.00928	0.029	-0.0014

IV. Results And Discussion

C. Analysis of Parametric influence on deviation of upper width

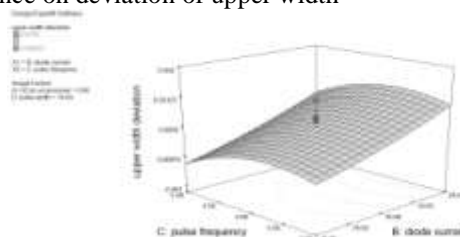


Fig.3 Surface response graph of Pulse frequency vs Diode current.

Fig.3 shows the combined effect of diode current and pulse frequency on deviation on upper width. It is clearly visible from the graph that as the input diode current increases then the upper width deviation increase owing to the fact that as the supply diode current increases then the pulse energy also increases so more material at the interaction zone melted and vaporized which leads to higher deviation in upper groove width. The deviation of upper width versus pulse frequency shows at first the deviation increases but after 4kHz frequency it declines rapidly due to the fact that initially when the no of pulses incident on the surface increases pulse overlapping increases which creates more concentrated energy and leads to increase in deviation of upper width but as the repetition frequency increases more than 4 kHz the pulse off time decreases which leads to less time for amplification to occur and average energy of pulse reduces so lesser area melts and evaporates and leads to lower deviation in upper width.

B. Effect of Pulse width and Current

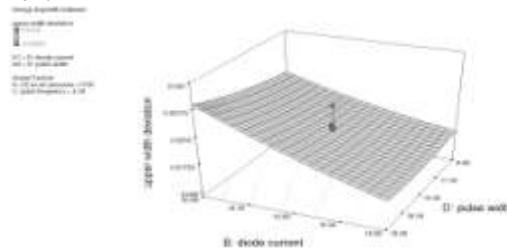


Fig.4 Surface response graph of Diode current vs Pulse width

Fig.4 shows the effect of current and pulse width on upper width deviation. It is observed that upper width deviation increases with the diode current irrespective of pulse width. The nature of variation of the upper width deviation with applied diode current is almost similar to the different pulse frequency and the nature of variation is almost linear. It is due to the fact that energy of laser beam mainly depends on diode current. High diode current develops high thermal energy, as a result of work sample where the laser beam is focused, get melted and vaporized instantly and large volume of material is removed from the top surface during penetration into the remaining thickness, which produces large upper width deviation. The low energy of laser beam generates small upper width deviation. From the response plot it has been observed that the upper width deviation almost linearly varies with pulse width. At very high pulse width, relatively large upper width deviation is observed but at low pulse width, low upper width deviation is seen. Because at low pulse width the peak power of the laser beam increases so high concentrated laser beam energy causes faster rate of penetration compared to high pulse width which in turn reduces the peak power, as a result less upper width deviation is formed.

C. Effect of Current VS Air Pressure

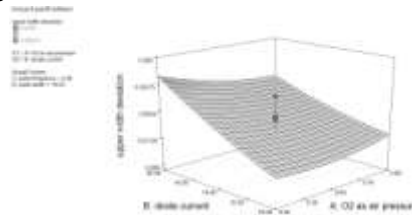


Fig.5 Surface response graph of Current vs Air pressure.

This graph shows the effect of diode current and oxygen and air pressure on upper width deviation. This has the same explanation as before, more energy more width but in presence of oxygen as assist gas creates oxidation reaction at high temperature which in turn releases more energy and this energy aids with beam energy. So much more surface gets melted and burning of side surface occurs which causes the upper width to increase and also the graph shows a stiff rapid increase in deviation but at a specific value of diode current as the air pressure increases it imposes a mechanical force on vaporized particles so a relative increase in upper width is achieved.

V. Effect Of Process Parameters On Deviation Of Depth

D. Effect of current vs air pressure

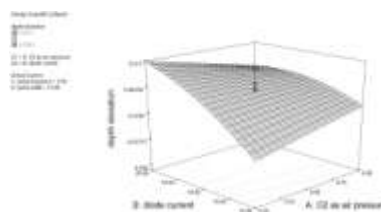


Fig.6 Surface response graph of Current vs Air pressure.

Fig.6 depicts that at any level values of pulse frequency the depth deviation increases with increase in diode current, this is due to the fact that has already been explained, as current increases the the energy of pulse increases which causes more thermal damage to the interaction surface and leads to more material evaporation which causes increase in depth. It is also clearly visible from the diagram that at high pulse frequency and high

current value the achieved depth deviation is high this is due to the fact that as the no of pulses incident on the same spot further increases the pulse overlap percentage also increases which in turn develops high vaporisation rate. High rate of vaporization imposes shockwave on material which again travels at a high speed to increase the depth.

E. Effect of pulse width vs pulse frequency on depth deviation

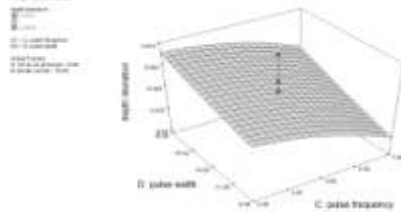


Fig.7 Surface response graph of Pulse Width vs Pulse frequency

Fig.7 shows the effect of pulse width and pulse frequency on depth deviation. It is clearly shown in the graph that as the pulse width increases the deviation in depth increases, due to the fact that the laser interaction surface gets more time for energy absorption which in turn increases the depth of the groove, so deviation linearly increases with pulse width. At any level of pulse width as the pulse frequency increases at first the deviation slightly increases but at high frequency value the deviation decreases this is due to the fact that as the pulse frequency increases the pulse off time reduces which in turn reduces the average power of laser because less time is available for achieving the amplification in laser cavity.

F. Effect of current vs air pressure for depth deviation

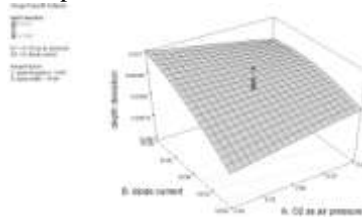


Fig.8 Surface response graph of Current vs Air pressure

This graph shows the combined effect of current and air pressure on depth deviation. As the current value is going to increase the depth deviation in turn increases. It was explained earlier high current high energy i.e. high pulse energy creates more thermal impact. Even if at low air pressure the graph showing the same effect because at low air pressure the mechanical force developed for drag the molten material is less. The deviation due to increase in air pressure also increases due to at high pressure of gas which induces more mechanical forces to drag out the molten materials which in turn increases the depth deviation.

2. EFFECT OF PROCESS PARAMETERS ON DEVIATION OF LOWER WIDTH

A. Effect of current vs air pressure

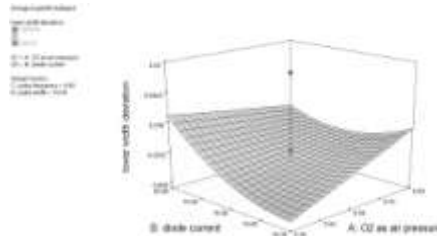


Fig.9 Surface response graph of Current vs Air pressure

Fig.9 demonstrates the effect of current and air pressure on lower width deviation. It was previously explained that as current increases the lower width deviation increases due to high energetic pulses coming from laser head. It was also found that at lower value of current and lower value of air pressure deviation is strictly minimal in nature, this is due to the fact that at low current value the machining surface gets less energy and also the deviation is minimum due to the vaporization of the upper portion of the material but the lower portion of the material is in a molten state which is not removed by the low pressure gas supply and leads towards decrease in lower width of the groove.

B. Pulse Frequency vs air Pressure

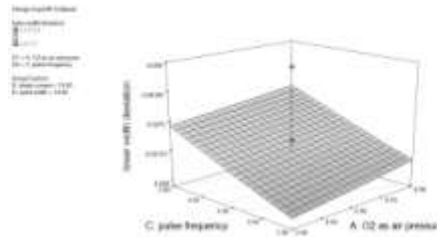


Fig.10 Surface response graph of Pulse frequency vs Air pressure

The graph shows the combined effect of pulse frequency and air pressure on lower width deviation. It is clearly visible that as the pulse frequency increases the lower width increases but as compared to the upper width, the increase in deviation is less. This is due to the fact that the beam intensity reduces to (1/e)% on changing the focal point, so less energetic pulses create less deviation, or this may be due to the fact that the gaussian beam shape, i.e. centre portion getting more energy as the beam profile moves towards the beam intensity decreases. Further, as the air pressure increases at all levels of current, it was shown that the deviation increases linearly, which is similar to the explanation given earlier that with the increase in gas pressure more mechanical force is induced on side surfaces which in turn increases the lower width but the deviation is less as compared to upper width deviation. This is due to the fact that at high current value the material that is vaporized creates a shock wave which is mainly opposite to gas pressure so due to that wave the material is not dragged out easily so lower width deviation is minimum as comparable to upper width deviation.

VI. Optimization By Pso(Particle Swamp Optimization)

The PSO algorithm was first introduced by Kennedy and Eberhart [13]. PSO is based on the social behaviour of animals and birds. It is influenced by the social behaviour in a flock of birds, school of fishes and a group of people. In PSO, the group is also known as swarm. It is a population-based stochastic optimization process. The swarm consists of number of individuals called the particles. These particles fly in a n-dimensional space. In PSO algorithm, the flight trajectory of a particle is influenced by the trajectory of neighbourhood particles as well as the flight experience of the particle itself. Each particle is treated as a point in the n-dimensional space. Each particle keeps information of its best coordinates in the problem space. These coordinates are the best solutions that the particle has achieved till that time. It is termed as pbest (personal best). The particle also keeps track of other particles in the neighbourhood. So, it is important to check whether there is any other particle in the neighbourhood that has better coordinates than this particle. If there is another particle with better coordinates than its coordinates, then that particle's coordinates are termed as local best, (lbest), otherwise, the coordinates of the considered particle are taken as the local best (lbest). Now, if this method is continued and all the particles individually are considered, the option of checking the coordinates of all the particles and changing the lbest and pbest values accordingly can be adopted. The particle with the best coordinate values after all the particles have been compared is termed as the global best value (gbest). This global best value gives the best solution of the optimization problem. Every particle has a velocity component and a position component. Say, for particle the position component is represented by xi and the velocity component is represented by vi. Now, this particle will keep on changing its velocity, along with which the position of the particle also changes. The velocity component is represented by vi = vi1,vi2,vi3,....., and the position component is represented by xi = xi1,xi2,....., . The particles change their velocity and position according to the following equation:

$$V_i^{k+1} = wV_i^k + c_1r_1(p_i - x_i^k) + c_2r_2(p_g - x_i^k) \dots \dots \dots (1.1)$$

$$x_i^{k+1} = x_i^k + V_i^{k+1} \dots \dots \dots (1.2)$$

where i = 1, 2, . . . ,N, N is the size of the population, w is the inertia weight, c1 and c2 are two positive constants, called the cognitive and social parameter respectively, and r1 and r2 are random numbers uniformly distributed within the range (0,1). The above equations are used to determine the new velocity and position of particle.

C. Single Response Optimization Result by PSO

In this section each objective function is taken separately for optimization. The respective optimal process parameter can be found out from the PSO mat lab coding. The equation for upper width, lower width & depth deviation has given in coded form as

$$Y_{UPWD} = .225 + .061X_1 - .0327X_2 + .0315X_3 - .00591X_4 + .0416X_1^2 + .00107X_2^2 - .00510X_3^2 + .000043X_4^2 - .01181X_1X_2 + .01905X_1X_3 + .00224X_1X_4 + .00039X_2X_3 + .00380X_2X_4 - .000893X_3X_4$$

$$Y_{LWD} = 1.391 + .259X_1 - .1229X_2 - .0304X_3 - .03644X_4 + .0019X_1^2 + .00286X_2^2 + .00017X_3^2 - .000163X_1X_2 - .0009X_1X_3 + .00415X_1X_4 + .00140X_2X_3 + .001501X_2X_4 + .000557X_3X_4$$

$$Y_{DD} = .225 + .061X_1 - .0327X_2 + .0315X_3 - .00591X_4 + .0416X_1^2 + .00107X_2^2 - .00510X_3^2 + .000043X_4^2 - .01181X_1X_2 + .01905X_1X_3 + .00224X_1X_4 + .00039X_2X_3 + .00380X_2X_4 - .000893X_3X_4$$

Table-8 showing the optimum response value from PSO

Responses	Optimize d value(mm)	X1 (air pressure) Kg/cm ²	X2 (diode current) Amp	X3 (Pulse frequency) kHz	X4 (Pulse width) %
Y _{UPWD}	.0079	1	19.74	2	4
Y _{LWD}	.0221	.2	17.67	2	21.2
Y _{DD}	-.0395	1	20.65	2	4

D. MOPSO (Multi-objective particle swarm optimization)

For multi-response optimization of Nd:YAG laser micro-grooving process, the following equation is developed considering both the responses simultaneously. so that all responses optimized and optimal parameter setting can be found out. Objective function given by ([14],[15]).

$$Z_{GLOBALMIN} = w_1 * \frac{Y_{UPWD}}{Y_{UPWDMIN}} + w_2 * \frac{Y_{DD}}{Y_{DDMIN}} + w_3 * \frac{Y_{LWD}}{Y_{LWDMIN}}$$

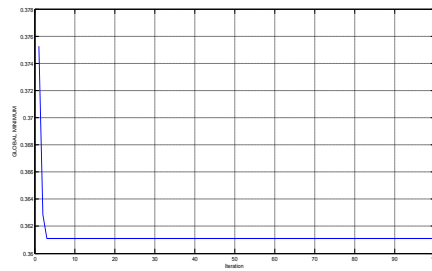
Range of values for input parameters are follows.

$$.2 < X_1 < 1, 17 < X_2 < 21, 2 < X_3 < 6, 4 < X_4 < 24$$

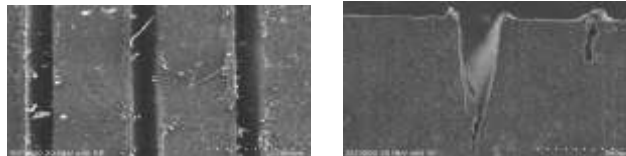
Weightage Condition $W_1 + W_2 + W_3 = 1$

$Y_{UPWD}, Y_{LWD}, Y_{DD}$ minimum values was found from the single response optimization. Here each objective function we have to minimize. So combining each objective function to a single objective function. Various grooves are machined by utilizing this optimal values and further measurement have done for responses. The actual and predicted values were compared to investigate the causes to reduce the deviation as much as possible. It was found that Z_{MIN} value .3611 is occurring at (.80 weightage to depth deviation, 10% equally importance to other 2 values. Finally at this values the corresponding parameter setting was found out and single grooving was carried out. The optimal parameter setting was found to be $x_1=1, x_2=19.02, x_3=2$ khz, $x_4=24\%$. by giving various weight-age to different response. Which having the lower Z_{min} value corresponding response value ie ($Y_{UPWD}, Y_{LWD}, Y_{DD}$) will be found out

Z _{min}	Response value			W ₁	W ₂	W ₃
	Y _{UPD}	Y _{LWD}	Y _{DD}			
1.0291	.0124	.0253	-.0172	.33	.33	.33
.84003	.0215	.0276	.0021	.50	.25	.25
1.0301	.0106	.0239	-.0247	.25	.50	.25
1.1447	.0326	.0339	.0151	.25	.25	.50
.3611	.0264	.0432	.01	.80	.10	.10
1.0087	.0113	.0225	-.0239	.10	.80	.10
1.0664	.0364	.0353	.0143	.10	.10	.80



Graph showing the optimal global min vs no of iteration



SEM image showing upper SEM-image showing the lower width and depth deviation surface of machined groove

VII. Conclusions

Experiments have been performed successfully to produce the desired micro-groove on Al-SiC composite by utilizing DPSS Nd:YAG laser operating on pulsed mode. The experiments were suitably conducted with the predefined range of process parameters according to the design of experiments to obtain the responses viz. upper width, lower width & depth deviation. The experimental analysis gives the following results:

For single response optimization to get the desired response within optimal value the set of parameter setting was found out. For minimum depth deviation it was found that air pressure of (1kgf/cm²), current value at 20.65 Amps, pulse frequency at 2 KHz and pulse width at 4% duty cycle. Likewise for upper width deviation the corresponding parameter setting was found to be 1kgf/cm², 19.74Amps, 2 KHz frequency and 4% duty cycle. Similarly for lower width deviation .2 as air pressure, 17.67 as current value 2KHz as frequency, 21.2 % as pulse width. By utilizing this single objective response value a multi-objective optimization technique was developed by assigning various weights to the responses and constructing a single objective function which in turn was optimized by PSO algorithm. Various weight criteria have been chosen to get the optimal value. Finally it was found that when 80% weightage has been given to depth deviation and 10% to the other two value of response which was found to be minimum. The optimal parameter setting was found to be X1=1, X2=19.02, X3=2 KHz, X4=24%. Further the convergence curve shows the less iteration was required to get the optimum value. Finally the micro-grooves were machined under optimal condition and the results were compared with the optimum result from PSO. It was found that the actual response value agrees with the predicted value with reasonably less error percentage.

It is clearly observed from the machined surface that the oxygen as a assist gas creates undesirable burning which in turn creates more defects. The SEM image also reveals That by taking low pressure assist gas the materials are not removed properly and also these ejaculated materials deposits on side surface to create recast like structure which is one of the undesirable defect developed.

One special defect observed inside the surface of the groove wall are irregular shape like particles remained on the sides of the wall and welded with it. This burr like defects can be removed by increasing the pulse frequency, but in the present work the range of pulse frequency chosen was not appropriate for a fine groove wall surface.

Further analysis can be carried to investigate the composition and thickness of the recast layer by utilizing EDX testing. So that optimal parameter combination can be found out for thickness of recast layer as a optimal response parameter. It was also found from the experiment that the precise groove dimension can be achieved if the heat affected area can be reduced. So a further simulation study was necessary to bring the temperature distribution inside the wall microstructure.

The predicted optimized responses agree with actual responses at optimal parameter settings. So the desired groove with high groove quality and desired tolerance level can be achieved. It was finally concluded from the experiment these undesirable effects may be reduced significantly if we take the current value, pulse frequency and air pressure more the range of value chosen here.

References

- [1]. Jain, V.K., Advanced Machining Processes, Allied Publishers Pvt. Ltd, New Delhi,2002.
- [2]. Ghosh, A. and Mallik, A.K., Manufacturing Science. East West Press Private Limited, New Delhi, 2008.
- [3]. Fundamentals of laser micromachining by Ronald. D.Schaeffer.
- [4]. Gilbert, Tod, Vladimir D. Krstic, and Gene Zak. "Machining of aluminium nitride with ultra-violet and near-infrared Nd: YAG lasers." Journal of materials processing technology 189.1 (2007): 409-417.
- [5]. Jain, R.K., Production Technology, Khanna Publishers, New Delhi, 2005.
- [6]. Gilbert, Tod, Vladimir D. Krstic, and Gene Zak. "Machining of aluminium nitride with ultra-violet and near-infrared Nd: YAG lasers." Journal of materials processing technology 189.1 (2007): 409-417.
- [7]. Reddy, A. Chennakesava, and Essa Zitoun. "Matrix Al-alloys for silicon carbide particle reinforced metal matrix composites." Indian journal of Science and Technology 3.12 (2010): 1184-1187.
- [8]. Yue, T. M., and W. S. Lau. "Pulsed Nd: YAG laser cutting of Al/Li/SiC metal matrix composites." Material and Manufacturing Process 11.1 (1996): 17-29.
- [9]. Cutting of 1.2mm thick austenitic stainless steel sheet using pulsed and CW Nd:YAG laser K. Abdel Ghany * , M. Newishy.
- [10]. Woo Chun Choi and George Chryssolouris: Analysis of the laser grooving and cutting processes: 1995 J. Phys. D: Appl. Phys. 28 873 .
- [11]. Montgomery, Douglas C. Design and analysis of experiments. John Wiley & Sons, 2008.
- [12]. D. Dhupal, B. Dolo, B. Bhattacharyya: Pulsed Nd:YAG laser turning of micro-groove on aluminum oxide ceramic (Al₂O₃): International Journal of Machine Tools & Manufacture 48 (2008) 236-248.
- [13]. <http://www.swarmintelligence.org/tutorial/> (accessed on 29th March, 2013).
- [14]. Mukherjee, Rajarshi, Debkalpa Goswami, and Shankar Chakraborty. "Parametric optimization of Nd: YAG laser beam machining process using artificial bee colony algorithm." Journal of Industrial Engineering 2013 (2013).
- [15]. Akay, B. and Karaboga, D., Artificial bee colony algorithm for large-scale problems and engineering design optimization, Journal of Intelligent Manufacturing, 23, 1001-1014, 2012.

Tatwa Prakash Pattasani "Experimentation And Optimization of Al-SiC based Metal Matrix Composite In Laser Micromahining" International Journal of Engineering Science Invention (IJESI), Vol. 04, No. 06, 2015, PP 106-116.